Geophysical Research Letters

RESEARCH LETTER
10.1029/2018GL078703

Key Points:
- Ocean model simulations of an idealized seamount in rotating, stratified flow show vertically decoupled vortex shedding
- Decoupled vortices tend to shed at a Strouhal number consistent with high Reynolds number flow past a cylinder
- The transition from uniform vortex shedding to a vertically varying shedding frequency is controlled by a critical Burger number

Correspondence to:
B. Perfect,
bperfect@uw.edu

Citation:
Perfect, B., Kumar, N., & Riley, J. J. (2018). Vortex structures in the wake of an idealized seamount in rotating, stratified flow. *Geophysical Research Letters*, *45*. https://doi.org/10.1029/2018GL078703

Received 9 MAY 2018
Accepted 21 AUG 2018
Accepted article online 29 AUG 2018

Vortex Structures in the Wake of an Idealized Seamount in Rotating, Stratified Flow

B. Perfect[1], **N. Kumar**[2], **and J. J. Riley**[1]

[1]Department of Mechanical Engineering, University of Washington, Seattle, WA, USA, [2]Department of Civil and Environmental Engineering, University of Washington, Seattle, WA, USA

Abstract We present the results of a 3-D computational model of an idealized seamount in rotating, stratified flow. The emergent vortex structures in the lee of the seamount indicate that the vertical coherence of vortices is strongly dependent on the Coriolis parameter and the background buoyancy frequency. A novel finding from this work is that above a critical Burger number the vortex shedding frequency varies vertically with the local seamount diameter and adjusts such that the Strouhal number based on the local seamount diameter is consistent with high Reynolds number flow past a circular cylinder. This study extends previous literature into a regime exhibiting stronger stratification and rotation, where the transition into vertically decoupled eddies occurs. Physically, this transition is associated with the loss of geostrophy in the eddies. The mechanisms governing the transition to vertically decoupled vortices may play an important role in the energetics of a seamount interacting with a barotropic flow.

Plain Language Summary We use an open-source ocean modeling code to explore the effects of the Earth's rotation and stratification on an oceanic flow past a mountain. Previous literature has reported that the entire mountain sheds eddies as a unit. However, we report that for strongly stratified flow with a relatively weak effect of rotation, the eddies do not shed as a unit but individually at different vertical levels. This effect is consistent with the flow behaving as many independent 2-D layers. It is possible to predict the transition from eddies shedding as a single unit to many independent levels using the relative strengths of the rotation and stratification. This prediction is well supported by physical arguments.

1. Introduction

1.1. Seamouts

Seamounts are an ubiquitous feature of Earth's oceans; it is estimated that there exist over 100,000 seamounts exceeding 1 km in height (Wessel et al., 2010). Theoretical scalings, field measurements, and model simulations demonstrate that seamounts play a significant role in ocean energetics (e.g., Melet et al., 2013; Nikurashin & Ferrari, 2011). Seamounts are associated with the generation of internal gravity waves, which may either propagate long distances before breaking or dissipate locally and contribute to enhanced diapycnal diffusivity near seamounts (Alford et al., 2015; Carter et al., 2006; Grisouard & Staquet, 2010; Kunze, 2003; Lamb, 2014; Simmons et al., 2004). Highly localized patches of intense diapycnal diffusivity appear to be the key to resolving the apparent paradox of missing vertical mixing identified by Munk (1966) and so correctly identifying the causes and locations of these patches is of great importance for global ocean models. A long-standing hypothesis with unknown origination (e.g., Munk & Wunsch, 1998) proposes that seamounts are the *stirring rods* of the ocean, which implies that the hydrodynamic wakes of seamounts might, along with internal wave generation, form a significant contribution to the role of seamounts in the ocean mixing balance. The current state of the literature has been unable to satisfactorily address this hypothesis, although there has been a recent surge in interest in this topic. Through observations and numerical simulations, island wakes have been shown to be energetic and with mesoscale vortex shedding (Dong et al., 2007; Dong & McWilliams, 2007; Tomczak, 1988), but these studies do not account for the three dimensionality in the vortex structures that has been observed in the vicinity of seamounts (Chen et al., 2015) and sloping headlands (Callendar et al., 2011; Canals et al., 2009; McCabe et al., 2006).

Hydrodynamic simulations of seamounts with realistic topography have demonstrated the ability to reproduce observed flow patterns at topography such as Fieberling Guyot (Beckmann & Haidvogel, 1997), Cato Island (Coutis & Middleton, 2002), and Madeira Archipelago (Caldeira & Sangrà, 2012), but confounding

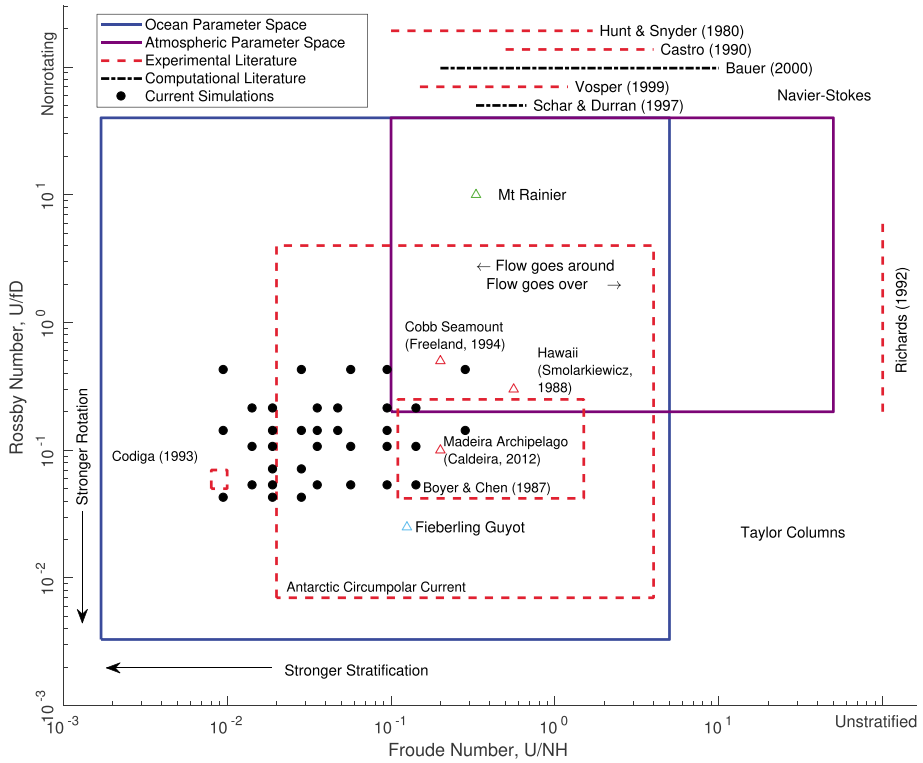

Figure 1. The dynamics of flow past a three-dimensional mountain can be plotted in a parameter space defined by the Froude and the Rossby numbers. Several key studies are indicated (Bauer et al., 2000; Caldeira & Sangrà, 2012; Castro et al., 1990; Freeland, 1994; Hunt & Snyder, 1980; Richards et al., 1992; Schär & Durran, 1997; Vosper et al., 1999), as well as the parameter spaces that might be observed in the ocean, atmosphere, and laboratory. Studies where the mountain dynamics are based on linear theory have not been plotted.

factors, such as complex density and current profiles, and irregular mountain shape have prevented these simulations from identifying the underlying mechanisms that produce the wake. Additionally, the presence of strong nonlinearities in these systems have resisted attempts to replicate observed currents near seamounts using analytical models (Brink, 1989, 1990). Individual seamounts cannot be resolved in Global Climate Models (Chen et al., 2013; Delworth et al., 2016), and so it is necessary to understand and parameterize the mechanisms controlling the wake structure and energetics rather than relying on the model to resolve them.

1.2. The Idealized Mountain

Even though hydrodynamic simulations of realistic seamounts are important tools for the analysis of field observations, here the focus is to determine the physical mechanisms associated with seamount wakes, which are better tracked through idealized simulations. The range of seamount heights being considered are such that the dynamics will be strongly nonlinear and outside the range of applicability of many thorough analytical models (Baines, 1995; Bell, 1975; Drazin, 1961). The geophysical application suggests that the wake structure will be governed, at least in part, by a Froude number and a Rossby number defined as

$$\mathrm{Fr} \equiv \frac{U}{NH} \qquad \mathrm{Ro} \equiv \frac{U}{fD}, \tag{1}$$

where U is a characteristic velocity, H is the seamount height, D is a characteristic seamount width, N is the Brunt-Väisälä frequency, and f is the Coriolis parameter.

Figure 1 provides a brief overview of literature involving flow past mountains, both in the atmosphere and in the oceans, organized by the range of Rossby and Froude numbers that were considered. Canals et al. (2009), in a study of tilted vortices in the wake of a sloping headland, motivate the need for a systematic study of hydrodynamic wakes in this parameter space. A significant number of studies with strong stratification did not consider rotation because they focused on terrestrial mountains, for which rotation is considered a secondary effect. However, the results are still relevant for the case of flow past seamounts. The case of strong

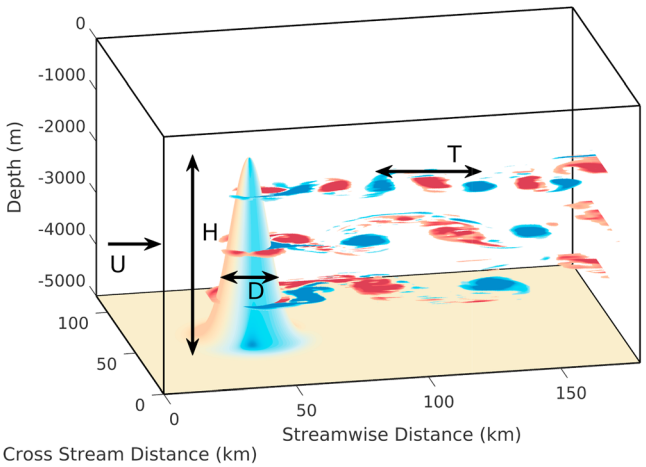

Figure 2. Schematic of the computational domain and inputs. A representative vortex shedding pattern is plotted using the vertical vorticity for several isopotential surface. A uniform velocity U and buoyancy frequency N are incident upon a mountain with characteristic height H and full width at half maximum D. Vortices are shed are with period T, which is indicated as the time separation between eddies with vorticity of like sign. An f-plane Coriolis parameter f is also present.

stratification and strong rotation (i.e., small Froude number and small Rossby number) is noticeably unpopulated, in part due to the challenges of achieving these conditions in a laboratory setting. This regime is also well outside of the dynamics observed in the atmosphere, though a potentially important one for the oceans, particularly in locations such as the Drake Passage.

2. Model Description and Methods

Idealized simulations were conducted using the Regional Ocean Modeling System (ROMS; Shchepetkin & McWilliams, 2005). ROMS is a free-surface, three-dimensional modeling framework that solves the primitive equations, with the hydrostatic and Boussinesq approximations. An axisymmetric 3,500-m Gaussian mountain with a full width at half maximum (FWHM) of 16.6 km is located within a prismatic domain. The domain is 180 km in the streamwise direction, 120 km in the cross stream direction, and 5,000 m deep (see Figure 2). The horizontal grid spacing is 1/3 km, and the model has 80 vertical terrain-following coordinates. The vertical grid stretching function is optimized for increased resolution near the bottom and middle of the water column, where the vortex shedding exists. The seamount is subjected to a uniform eastward flow $U = 0.1$ m/s, and the stratification is linear, producing a uniform background Brunt-Väisälä frequency N. An f-plane rotation term with magnitude f is included. Open-type boundary conditions are used, which are designed to radiate disturbances out of the domain with minimal reflection. The free surface is governed by a geostrophic balance in order to maintain the uniform eastward flow. No other atmospheric or boundary forcing was considered.

In the model setup (see Figure 2), we consider the seamount height H, the seamount FWHM D, the vertically varying seamount diameter $D'(z)$, a model viscosity ν, and a spatially varying vortex shedding period $T'(z)$. An application of the Buckingham Pi theorem suggests a set of nondimensional parameters as follows: a bulk Rossby number $\mathrm{Ro} \equiv \frac{U}{fD}$, the Froude number $\mathrm{Fr} \equiv \frac{U}{NH}$, the Reynolds number $\mathrm{Re} \equiv \frac{UD}{\nu}$, and the depth-varying Strouhal number $\mathrm{St}' \equiv \frac{D'(z)}{UT'(z)}$. The ratio of seamount height to ocean depth has been demonstrated to be an important parameter as well (Boyer & Chen, 1987), particularly for the internal wave and rotationally dominated regimes, but variation in this parameter will be neglected for this study. In general, the Rossby number will vary with the seamount diameter and therefore be depth dependent, but these variations are considered to be secondary with respect to the first-order dynamics. For a sufficiently high Reynolds number, the wake dynamics of the flow, measured as St', will be determined by Fr and Ro.

The physical dimensions of the model are fixed, so N and f are manipulated in order to vary Fr and Ro. A total of 35 simulations were run, spanning values of N from 1×10^{-4} to 3×10^{-3} s^{-1}, and values of f from 10^{-5} to 10^{-4} s^{-1}. Each simulation was run for approximately 80 days after an initial startup period, allowing the model to achieve a pseudoperiodic state. The run time was chosen such that at least eight Strouhal periods were captured. The model uses a $k - \epsilon$ closure scheme and a quadratic drag law with a constant drag coefficient of 2×10^{-3}. Model runs with a free slip bottom boundary condition still produced vortex shedding by baroclinic mechanisms, but the vortices tended to be weaker and less coherent. Sensitivity studies were conducted by varying the grid size, bottom drag coefficient, and horizontal viscosity formulation (harmonic and biharmonic) and magnitude. Results indicate that qualitative shedding patterns and primary-order energetics are relatively insensitive to grid spacing and bottom drag coefficient. A nominal horizontal fluid kinematic viscosity was used in order to obtain model stability. Using the criteria established by Dong et al. (2007), the effective Reynolds number (based on the seamount FWHM) was approximately 2,000.

The Strouhal number is computed from an ensemble of time series of relative vorticity in the vertical direction. For each group of points at the same vertical level, the spectral density estimations of each time series are summed and then the peak frequency (after excluding harmonics) is reported as the frequency of eddy shedding.

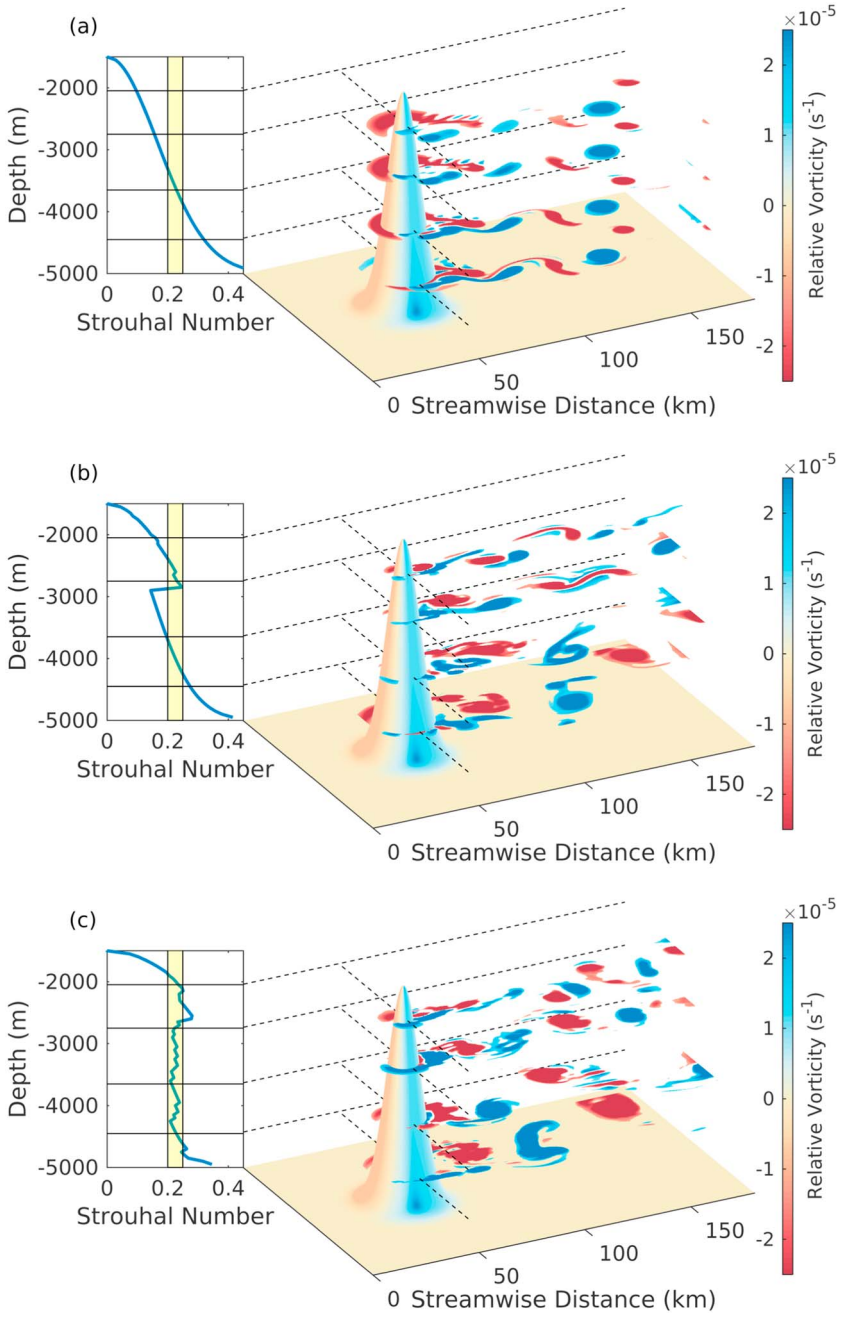

Figure 3. Results from three simulations are presented, which exhibit typical cases of the shedding regimes that were produced. Horizontal slices of the vertical vorticity are overlaid on the topography. In the top case (Ro = 0.14, Fr = 0.095), vortices are vertically aligned. The middle case (Ro = 0.14, Fr = 0.048) is a transitional regime, characterized by two regions of uniform shedding, separated by an interface where the shedding frequency changes abruptly. In the bottom case (Ro = 0.42, Fr = 0.029), vortices are fully decoupled. The vertically varying Strouhal numbers are indicated to the left, with a typical Strouhal number for high Re flow highlighted.

3. Vertical Vortex Structure

When subjected to uniform flow, the seamount produces a hydrodynamic wake. In most cases, the wake takes the form of coherent vortices, as illustrated in Figure 3. In the limiting case of large Fr and large Ro (i.e., tending toward nonrotating, unstratified flow), the wake exhibits 3-D turbulence, which prevents the formation of coherent vertically oriented vortices (Barkley & Henderson, 1996). This type of wake structure will not be discussed, in favor of the larger vortex structures that form in rotating, stratified flow. While the wake

structure may bear some resemblance to previous stratified wake studies (e.g., Billant & Chomaz, 2001; Lilly, 1983; Spedding, 1997), the additional effect of rotation produces a fundamentally different scaling behavior, which is discussed in section 4.

The vertical structure of the vortices may be categorized into two regimes, separated by a small transitional regime. The first regime (shown in the top plot of Figure 3 and characterized by weak stratification and strong rotation) exhibits vortex lines that are vertical or slightly tilted, extending from the bottom boundary layer up to the level of the seamount summit. Vortices are shed in a vertically uniform manner, resulting in a uniform shedding frequency at all elevations on the seamount. The Strouhal number, based on the local seamount diameter, therefore varies significantly over the height of the seamount. The vortex lines produced by this shedding are not Taylor columns because they do not necessarily extend beyond the seamount summit, with the distinction of being controlled by the ratio of seamount height to water depth (Boyer & Chen, 1987). These structures are consistent with the results of the laboratory experiments in Figure 1 (Castro et al., 1990; Hunt & Snyder, 1980).

In the second regime, characterized by strong stratification and weak rotation, vortices become decoupled in the vertical direction (see Figure 3c). That is, rather than each vortex shedding as a vertical unit, each seamount elevation sheds vortices independently. The shedding frequency varies strongly with depth, with the bottom of the seamount shedding at roughly an 8-day period, and the seamount summit shedding at 3- to 4-day intervals. Vortex lines may have significant vertical extent, but as suggested by Canals et al. (2009), the sloping seamount flank causes them to become strongly tilted with successive shedding periods, ultimately breaking down. The strongly time-dependent nature of this process resists a vertical length scale for the decoupled vortices, though it is clear that the effect of rotation allows their vertical extent to exceed the $\mathrm{Fr} = 1$ scaling seen in systems with only stratification (Billant & Chomaz, 2001; Lilly, 1983).

The bottom plot of Figure 3 gives insight into the distribution of shedding frequency; the vertical decoupling of eddies works to preserve a relatively constant Strouhal number. This Strouhal number matches the behavior observed for high Reynolds number flow past a circular cylinder (Zdravkovich, 1997). Therefore, averaged over the length of the simulation, each vertical level acts somewhat independently, almost as a two-dimensional plane. The type of vortex shedding produced in this regime has not been reported in literature, although Figure 1 suggests that this may be due to the regime lying outside of the parameter space that has previously been investigated.

A transitional regime, indicated in Figure 3b, separates the two shedding behaviors. Rather than varying continuously, the shedding frequency exhibits a small, finite number of jumps, separated by regions of uniformity. In the following section, we will discuss the mechanisms responsible for the transition from a vertically varying to a vertically uniform Strouhal number.

4. Discussion

Vertically decoupled vortices have not been reported for flow past three-dimensional obstacles in stratified flow. The parameter range in which this behavior exists is relatively unexplored and difficult to achieve in a laboratory setting (Vosper et al., 1999). Experiments have typically been limited to a small, finite number of inertial periods (Codiga, 1993), corresponding to few Strouhal periods. This may not be a long enough time for the vortex tilting to produce truly decoupled vortices, as startup effects in the simulations often produced several shedding periods of vertically uniform shedding before the vortices began to decouple.

The 35 simulations that were carried out have been plotted in the rotation-stratification parameter space in Figure 4. The decoupled shedding regime is characterized by weak rotation and strong stratification (high Ro and low Fr), and the coupled shedding regime exists where rotation is strong and stratification is weak (low Ro and high Fr). A proposed mechanism to predict vertically decoupled vortices is in terms of a critical Burger number, where the Burger number is defined by $\mathrm{Bu} \equiv \left(\frac{\mathrm{Ro}}{\mathrm{Fr}}\right)^2$ The transitional regime appears to lie in the range,

$$5.5 < \mathrm{Bu}_{\mathrm{crit}} < 12. \tag{2}$$

The Burger number is understood to have dynamical importance in distinguishing barotropic and baroclinic dynamics, where a larger Burger number is associated with barotropic flow (e.g., stronger stratification

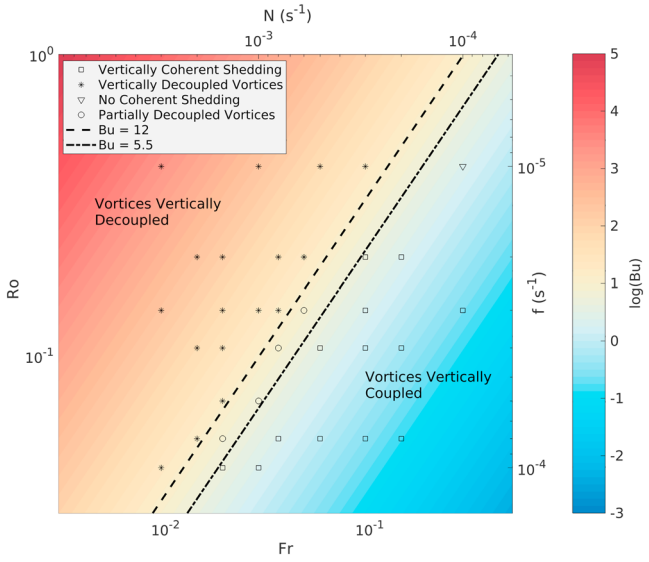

Figure 4. A summary of the simulations, with the regime of vortex shedding indicated as follows: Vertically uniform shedding is indicated by squares, vertically decoupled shedding is indicated by stars, and the transitional regime is indicated by circles. The triangle symbol (top right) is a case where coherent vortices never formed. The interface between uniform and decoupled shedding is indicated by lines of constant Burger number.

discourages the perturbation of isopycnals; Boutov et al., 2010). Another interpretation of this finding is that the Burger number scales as

$$\mathrm{Bu} \propto \left(\frac{R_d}{D}\right)^2, \tag{3}$$

where R_d is the first baroclinic Rossby radius of deformation, defined as $R_d \equiv \frac{NH}{\pi f}$ (Gill, 1982). Here H is the water depth for a uniformly stratified ocean. Dritschel and De La Torre Juârez (1996) suggest that the appropriate vertical length scale is the vertical extent of the eddies, which would mean that the controlling parameter would be

$$\left(\frac{R_d}{D}\frac{H_{\mathrm{seamount}}}{H_{\mathrm{depth}}}\right)^2. \tag{4}$$

For the simulations conducted here, $\frac{H_{\mathrm{seamount}}}{H_{\mathrm{depth}}}$ is held constant and it is of order 1, so we are not able to distinguish between the cases described by equations (3) and (4). However, our convergence tests suggest that equation (4) is the appropriate scaling, in line with Dritschel and De La Torre Juârez (1996). The critical Burger number is achieved when R_d surpasses the horizontal length scale of the seamount. If the horizontal length scale is taken to be $D/2$ to correspond to the deformation radius, then the critical Burger number is predicted to be

$$\mathrm{Bu}_{\mathrm{crit}} = \left(\frac{\pi}{2}\right)^2 \approx 2.5. \tag{5}$$

The critical Burger number predicted from equation (5) is somewhat smaller than the transitional Burger number identified in equation (2) from the simulations conducted here, but it is likely influenced by a number of factors. The predicted $\mathrm{Bu}_{\mathrm{crit}}$ is based on Gill's definition of L_R, and its comparison to the seamount radius (which is related to the vortex radius); other analyses have compared L_R to the vortex diameter (Dritschel et al., 1999) and used a definition for L_R that differs by a factor of π (Dong et al., 2007; Stegner & Dritschel, 2000). The predicted critical Burger number is therefore sensitive to different interpretations of L_R and the choice of horizontal length scale. Secondary effects include the Gaussian shape of the seamount and the influence of the bottom boundary layer. Higher-mode baroclinic Rossby numbers may also play a role in the transition process, but the transition onset appears to be dictated by the first mode. The Burger number associated with the nth baroclinic Rossby radius scales as n^2, and so leading-order influence of the second mode would imply a wider range of critical Burger number than is observed. Dritschel et al. (1999), in a numerical study of idealized vortices in rotating, stratified flow, report a shift in vortex dynamics at around $\mathrm{Bu} = 4$. The vortices were found to be subject to the *tall column instability* at large Bu, causing the breakdown of 2-D dynamics.

Previous studies have shown that the horizontal extent of eddies in rotating, stratified flow scales with the minimum of R_d and D and that behavior is also observed in the present study (Dong et al., 2007; Stegner & Dritschel, 2000). When $R_d < D$, the eddies are driven by a geostrophic balance and the dynamics are characterized by baroclinic flow (Boutov et al., 2010). Conversely, when $D < R_d$, the eddies lose geostrophic balance and behave in a manner more consistent with a classical barotropic wake. The horizontal extent of the eddies now scales with the local diameter of the seamount, and the shedding frequency is characterized by a constant Strouhal number.

5. Conclusions

We have documented a novel vortex shedding regime for rotating, stratified flow past a seamount using a ROMS model. In this regime, coherent vortices form and advect in a manner such that the different vertical levels do not affect one another. The transition from geostrophic, vertically coupled coherent vortices to an ageostrophic, uncoupled regime is well predicted by a critical Burger number. The physical interpretation of this finding is that when the baroclinic deformation radius exceeds the horizontal extent of the seamount, the flow tends to become barotropic, which permits a more classical 2-D wake structure to form. Once the eddies

are not constrained by rotational effects, the shedding frequency adjusts to produce a constant Strouhal number at all depths.

The vertically decoupled shedding regime may have important implications for the energetics of seamount interaction with currents, because the visually remarkable transition is accompanied by changes in the underlying dynamics from geostrophic to ageostrophic motion. Furthermore, Dong et al. (2007) and Stegner and Dritschel (2000) suggest that an important transition in the 2-D stability and energetics of nearly geostrophic vortices is associated with $\frac{Bu}{Ro}$ rather than Bu. A detailed energy analysis of the vertically decoupled vortex shedding mode may provide insight into the relative energetic importance of the decoupling versus the loss of 2-D stability.

Acknowledgments
This work was facilitated though the use of advanced computational, storage, and networking infrastructure provided by the Hyak supercomputer system and funded by the STF at the University of Washington. B. Perfect would like to thank B. Blakeley for productive conversation. N. Kumar acknowledges support from the Office of Naval Research, Littoral and Geosciences Division. J. J. Riley acknowledges support from PACCAR. The numerical code used for this work is open source and located at myroms.org. The postprocessed data set and model settings used to produce the above results are available through the Open Science Framework at osf.io/ntscf. Raw model simulations are archived and will be provided upon request by the corresponding author.

References

Alford, M. H., Peacock, T., MacKinnon, J. A., Nash, J. D., Buijsman, M. C., Centuroni, L. R., et al. (2015). The formation and fate of internal waves in the South China Sea. *Nature*, *521*(7550), 65–9. https://doi.org/10.1038/nature14399

Baines, P. G. (1995). *Topographic effects in stratified flows* (482 pp.). New York, NY: Cambridge University Press.

Barkley, D., & Henderson, R. (1996). Three-dimensional Floquet stability analysis of the wake of a circular cylinder. *Journal of Fluid Mechanics*, *322*, 215–241.

Bauer, M. H., Mayr, G. J., Vergeiner, I., & Pichler, H. (2000). Strongly nonlinear flow over and around a three-dimensional mountain as a function of the horizontal aspect ratio. *Journal of the Atmospheric Sciences*, *57*(24), 3971–3991.

Beckmann, A., & Haidvogel, D. B. (1997). A numerical simulation of flow at Fieberling Guyot. *Journal of Geophysical Research*, *102*(C3), 5595–5613. https://doi.org/10.1029/96JC03414

Bell, T. H. (1975). Lee waves in stratified flows with simple harmonic time dependence. *Journal of Fluid Mechanics*, *67*(4), 705–722. https://doi.org/10.1017/S0022112075000560

Billant, P., & Chomaz, J.-M. (2001). Self-similarity of strongly stratified inviscid flows. *Physics of Fluids*, *13*(6), 1645–1651. https://doi.org/10.1063/1.1369125

Boutov, D., Santos, A., Luís, E., & Videman, J. (2010). Numerical modeling of vorticity dynamics in oceanic wakes. In *V European Conference on Computational Fluid Dynamics* (pp. 14–17).

Boyer, D. L., & Chen, R.-R. (1987). Laboratory simulation of mountain effects on large-scale atmospheric motion systems. The Rocky Mountains. *Journal of the Atmospheric Sciences*, *44*(1), 100–123.

Brink, K. H. (1989). The effect of stratification on seamount-trapped waves. *Deep Sea Research Part A, Oceanographic Research Papers*, *36*(6), 825–844. https://doi.org/10.1016/0198-0149(89)90031-9

Brink, K. H. (1990). On the generation of seamount-trapped waves. *Deep Sea Research Part A, Oceanographic Research Papers*, *37*(10), 1569–1582. https://doi.org/10.1016/0198-0149(90)90062-Z

Caldeira, M., & Sangrà, P. (2012). Complex geophysical wake flows Madeira Archipelago case study. *Ocean Dynamics*, *62*(5), 683–700. https://doi.org/10.1007/s10236-012-0528-6

Callendar, W., Klymak, J. M., & Foreman, M. G. G. (2011). Tidal generation of large sub-mesoscale eddy dipoles. *Ocean Science*, *7*(4), 487–502. https://doi.org/10.5194/os-7-487-2011

Canals, M., Pawlak, G., & MacCready, P. (2009). Tilted baroclinic tidal vortices. *Journal of Physical Oceanography*, *39*(2), 333–350. https://doi.org/10.1175/2008JPO3954.1

Carter, G. S., Gregg, M. C., & Merrifield, M. A. (2006). Flow and mixing around a small seamount on Kaena Ridge, Hawaii. *Journal of Physical Oceanography*, *36*(6), 1036–1052. https://doi.org/10.1175/JPO2924.1

Castro, I. P., Snyder, W. H., & Baines, P. G. (1990). Obstacle drag in stratified flow. *Proceedings of the Royal Society of London*, *429*, 119–140. https://doi.org/10.1098/rspa.1983.0054

Chen, J.-H., Lin, S.-J., Chen, J.-H., & Lin, S.-J. (2013). Seasonal predictions of tropical cyclones using a 25-km-resolution general circulation model. *Journal of Climate*, *26*(2), 380–398. https://doi.org/10.1175/JCLI-D-12-00061.1

Chen, G., Wang, D., Dong, C., Zu, T., Xue, H., Shu, Y., et al. (2015). Observed deep energetic eddies by seamount wake. *Scientific Reports*, *5*, 17416. https://doi.org/10.1038/srep17416

Codiga, D. L. (1993). Laboratory realizations of stratified seamount-trapped waves. *Journal of Physical Oceanography*, *23*(9), 2053–2071. https://doi.org/10.1175/1520-0485(1993)023<2053:LROSST>2.0.CO;2

Coutis, P. F., & Middleton, J. H. (2002). The physical and biological impact of a small island wake in the deep ocean. *Deep-Sea Research I*, *49*, 1341–1361.

Delworth, T. L., Zeng, F., Vecchi, G. A., Yang, X., Zhang, L., & Zhang, R. (2016). The North Atlantic Oscillation as a driver of rapid climate change in the Northern Hemisphere. *Nature Geoscience*, *9*(7), 509–512. https://doi.org/10.1038/ngeo2738

Dong, C., & McWilliams, J. C. (2007). A numerical study of island wakes in the Southern California Bight. *Continental Shelf Research*, *27*(9), 1233–1248. https://doi.org/10.1016/j.csr.2007.01.016

Dong, C., McWilliams, J. C., & Shchepetkin, A. F. (2007). Island wakes in deep water. *Journal of Physical Oceanography*, *37*(4), 962–981. https://doi.org/10.1175/JPO3047.1

Drazin, B. P. G. (1961). On the steady flow of a fluid of variable density past an object. *Tellus*, *13*, 238.

Dritschel, D. G., & De La Torre Juârez, M. (1996). The instability and breakdown of tall columnar vortices in a quasi-geostrophic fluid. *Journal of Fluid Mechanics*, *328*, 129–160. https://doi.org/10.1017/S0022112096008671

Dritschel, D. G., De La Torre Juârez, M., & Ambaum, M. H. (1999). The three-dimensional vortical nature of atmospheric and oceanic turbulent flows. *Physics of Fluids*, *11*(6), 1512–1520. https://doi.org/10.1063/1.870014

Freeland, H. (1994). Ocean circulation at and near Cobb Seamount. *Deep-Sea Research I*, *41*(11/12), 1715–1732.

Gill, A. E. (1982). *Atmosphere-ocean dynamics* (662 pp.). San Diego, CA: Academic Press.

Grisouard, N., & Staquet, C. (2010). Numerical simulations of the local generation of internal solitary waves in the Bay of Biscay. *Nonlinear Processes in Geophysics*, *17*(5), 575–584. https://doi.org/10.5194/npg-17-575-2010

Hunt, J. C. R., & Snyder, W. H. (1980). Experiments on stably and neutrally stratified flow over a model three-dimensional hill. *Journal of Fluid Mechanics*, *96*(4), 671–704. https://doi.org/10.1017/S0022112080002303

Kunze, E. (2003). Yes, we have no abyssal mixing. In D. Muller & D. Henderson (Eds.), *Near-boundary processes and their parameterization* (pp. 85–93). Honolulu: University of Hawai'i at Monoa.

Lamb, K. G. (2014). Internal wave breaking and dissipation mechanisms on the continental slope/shelf. *Annual Review of Fluid Mechanics*, *46*(1), 231–254. https://doi.org/10.1146/annurev-fluid-011212-140701

Lilly, D. K. (1983). Stratified turbulence and the mesoscale variability of the atmosphere. *Journal of the Atmospheric Sciences*, *40*(3), 749–761. https://doi.org/10.1175/1520-0469(1983)040<0749:STATMV>2.0.CO;2

McCabe, R. M., MacCready, P., Pawlak, G., McCabe, R. M., MacCready, P., & Pawlak, G. (2006). Form drag due to flow separation at a headland. *Journal of Physical Oceanography*, *36*(11), 2136–2152. https://doi.org/10.1175/JPO2966.1

Melet, A., Nikurashin, M., Muller, C., Falahat, S., Nycander, J., Timko, P. G., et al. (2013). Internal tide generation by abyssal hills using analytical theory. *Journal of Geophysical Research: Oceans*, *118*, 6303–6318. https://doi.org/10.1002/2013JC009212

Munk, W. (1966). Abyssal recipes. *Deep-Sea Research*, *13*, 707–730.

Munk, W., & Wunsch, C. (1998). Abyssal recipes II. *Deep-Sea Research I*, *45*, 1977–2010.

Nikurashin, M., & Ferrari, R. (2011). Global energy conversion rate from geostrophic flows into internal lee waves in the deep ocean. *Geophysical Research Letters*, *38*, L08610. https://doi.org/10.1029/2011GL046576

Richards, K. J., Hopfinger, E. J., & D'hières, G. C. (1992). Boundary-layer separation of rotating flows past surface-mounted obstacles. *Journal of Fluid Mechanics*, *237*, 343–371. https://doi.org/10.1017/S0022112092003446

Schär, C., & Durran, D. R. (1997). Vortex formation and vortex shedding in continuously stratified flows past isolated topography. *Journal of the Atmospheric Sciences*, *54*, 534–554. https://doi.org/10.1175/1520-0469(1997)054<0534:VFAVSI>2.0.CO;2

Shchepetkin, A. F., & McWilliams, J. C. (2005). The Regional Ocean Modeling System: A split-explicit, free-surface, topography following coordinates ocean model. *Ocean Modelling*, *9*, 347–404. https://doi.org/10.1016/j.ocemod.2004.08.002

Simmons, H., Hallberg, R. W., & Arbic, B. K. (2004). Internal wave generation in a global baroclinic tide model. *Deep Sea Research Part II: Topical Studies in Oceanography*, *51*(25-26), 3043–3068. https://doi.org/10.1016/j.dsr2.2004.09.015

Spedding, G. R. (1997). The evolution of initially turbulent bluff-body wakes at high internal Froude number. *Journal of Fluid Mechanics*, *337*, 283–301. https://doi.org/10.1017/S0022112096004557

Stegner, A., & Dritschel, D. G. (2000). A numerical investigation of the stability of isolated shallow water vortices. *Journal of Physical Oceanography*, *30*(10), 2562–2573. https://doi.org/10.1175/1520-0485(2000)030<2562:ANIOTS>2.0.CO;2

Tomczak, M. (1988). Island wakes in deep and shallow water. *Journal of Geophysical Research*, *93*(C5), 5153–5154. https://doi.org/10.1029/JC093iC05p05153

Vosper, S. B., Castro, I. P., Snyder, W. H., & Mobbs, S. D. (1999). Experimental studies of strongly stratified flow past three-dimensional orography. *Journal of Fluid Mechanics*, *390*, 223–249. https://doi.org/10.1017/S0022112099005133

Wessel, P., Sandwell, D., & Kim, S.-S. (2010). The global seamount census. *Oceanography*, *23*, 24–33. https://doi.org/10.5670/oceanog.2010.60

Zdravkovich, M. M. (1997). *Flow around circular cylinders: A comprehensive guide through flow phenomena, experiments, applications, mathematical models, and computer simulations* (Vol. 1, 672 pp.).